



This is a repository copy of *Localised variations in reflected pressure from explosives buried in uniform and well-graded soils.*

White Rose Research Online URL for this paper:  
<http://eprints.whiterose.ac.uk/105010/>

Version: Accepted Version

---

**Proceedings Paper:**

Rigby, S.E., Fay, S.D., Tyas, A. et al. (5 more authors) (2016) Localised variations in reflected pressure from explosives buried in uniform and well-graded soils. In: Proceedings of the 24th Military Aspects of Blast and Shock. 24th Military Aspects of Blast and Shock, 19-23 Sep 2016, Halifax, Nova Scotia, Canada. MABS .

---

**Reuse**

Unless indicated otherwise, fulltext items are protected by copyright with all rights reserved. The copyright exception in section 29 of the Copyright, Designs and Patents Act 1988 allows the making of a single copy solely for the purpose of non-commercial research or private study within the limits of fair dealing. The publisher or other rights-holder may allow further reproduction and re-use of this version - refer to the White Rose Research Online record for this item. Where records identify the publisher as the copyright holder, users can verify any specific terms of use on the publisher's website.

**Takedown**

If you consider content in White Rose Research Online to be in breach of UK law, please notify us by emailing [eprints@whiterose.ac.uk](mailto:eprints@whiterose.ac.uk) including the URL of the record and the reason for the withdrawal request.



[eprints@whiterose.ac.uk](mailto:eprints@whiterose.ac.uk)  
<https://eprints.whiterose.ac.uk/>

# LOCALISED VARIATIONS IN REFLECTED PRESSURE FROM EXPLOSIVES BURIED IN UNIFORM AND WELL-GRADED SOILS

S. E. Rigby<sup>1</sup>, S. D. Fay<sup>1,2</sup>, A. Tyas<sup>1,2</sup>, S. D. Clarke<sup>1</sup>, J. J. Reay<sup>2</sup>, J. A. Warren<sup>1,2</sup>, M. Gant<sup>3</sup>,  
I. Elgy<sup>3</sup>

<sup>1</sup>*Department of Civil & Structural Engineering, University of Sheffield, Mappin Street, Sheffield, S1 3JD, UK;*

<sup>2</sup>*Blastech Ltd., The BioIncubator, 40 Leavygreave Road, Sheffield, S3 7RD, UK;*

<sup>3</sup>*Defence Science and Technology Laboratory (Dstl), Porton Down, Salisbury, Wiltshire, SP4 0JQ, UK.*

## ABSTRACT

Recent experiments into characterisation of the loading resulting from detonation of a shallow buried explosive have highlighted the complex underlying physical mechanisms present at the face of a target situated above the soil surface. This paper presents the results from such experiments, where the localised blast pressure and impulse is measured using an array of Hopkinson pressure bars at specific points on the target surface. Two different soil types are tested; a relatively uniform sand, and well-graded sandy-gravel. It is observed that the variability in localised loading is intrinsically linked to the particle size distribution of the soil medium; the uniform soil produces repeatable data with little variation whereas the well-graded soil demonstrates considerable spread. The cause of this spread is quantified and discussed with reference to the distinct loading mechanisms acting on the target as seen in the experimental data.

## INTRODUCTION

Buried improvised explosive devices (IEDs) and landmines are common throughout areas of conflict. The amplification of blast pressures caused by the surrounding soil, plus the difficulties associated with detecting and clearing buried explosives, makes the landmine a very powerful and dangerous weapon. According to the 2015 *Landmine Monitor* report there were 3,678 recorded casualties from victim-activated landmines, buried IEDs, cluster munition remnants and explosive remnants of war worldwide in the year 2014 alone. Since 1999 there have been almost 100,000 deaths from such weapons [1].

The subject of quantification of the effect of buried explosions on above-ground structures began to gather interest in North America in the 1970s and 1980s [2–4], culminating in the work of Bergeron et al. [5]. Whilst these early experimental studies implemented a variety of diagnostic techniques, until recently the exact detail of both the spatial and temporal distribution of loading has been immeasurable.

The problem of the lack of robust experimentation for measuring the pressure output from buried explosives was initially addressed by the small-scale testing conducted at the University of Maryland, USA [6], and more recently by the quarter-scale apparatus developed by the current authors [7]. It is known that the properties of the surrounding soil are key to determining the output from buried explosives [8]. This paper details the results from tests using two different soil types, each with a distinct particle size distribution, to assess the influence of uniformity of the surrounding soil on the localised variations in reflected pressures from shallow buried explosives.

## APPARATUS

The apparatus used in the current study is housed at the University of Sheffield explosive testing facility in Buxton, Derbyshire, UK, and is described in detail in Ref. [7]. The test rig consists of two large, reinforced concrete reaction frames (Figure 1a), placed approximately 700 mm apart. Directly underneath the midpoint of the reaction structure sits a steel container, made from 30 mm thick steel plate and formed into a 500 mm diameter, 375 mm high open-top cylinder (Figure 1b). This container is filled with soil and a cylindrical, 78 g PE4 charge is buried to a depth of 28 mm, according to the methodology outlined in Ref. [9], where the burial depth is given as the distance from the soil surface to the top of the charge, as in Figure 1b.

The charge is encased in a 3 mm thick PVC container with no lid, and is similar to a quarter-scale version of STANAG threat level M2b, as given in the Allied Engineering Publication *Procedures for evaluating the protection level of logistic and light armoured vehicles (AEP-55)* [10], which is itself a testing addenda to NATO standardisation agreement, STANAG 4569 [13]. The full-scale threat is specified as 6 kg TNT. In the current study, this has been replaced with a 5 kg PE4 charge assuming a TNT equivalence of 1.2 after work by the current authors [11] as PE4 exhibits more repeatable detonation behaviour and is also more stable than TNT.

A 1400 mm diameter, 100 mm thick steel target plate is attached to the underside of the reaction frames (via load cells attached to a steel ‘acceptor’ plate which is cast into the concrete) and spans between them. The centre of the plate is directly in line with the centre of the soil container, and 140 mm above the plane of the top of the container (i.e. the soil surface). A series of 10.5 mm holes are drilled through the thickness of the target plate; in four arrays emanating from the plate centre at 25 mm centre-to-centre spacing, perpendicular and parallel to the span of the plate, with a central hole common to all four arrays (Figure 1c). The arrays to the left and right of the central hole (in plan) are termed the  $-x$  and  $+x$  arrays, and those below and above the central hole (in plan) are termed the  $-y$  and  $+y$  arrays. Here, the plate spans in the  $y$  direction.

Through each of these holes, 10 mm diameter, 3.25 m long EN24(T) steel Hopkinson pressure bars (HPBs) [12] are inserted from above. The HPBs are suspended from a receiver frame placed atop the main reaction frame, and are machined with threaded ends to allow for fine adjustments to their height to ensure that the face of each HPB sits flush with the loaded face of the target plate. Semi-conductor strain gauges are mounted in pairs on the perimeter of each HPB, 250 mm from the loaded face, in a Wheatstone-bridge circuit to ensure that only the axial strain component was recorded. The pressure acting on the face of each bar, and hence the temporal and spatial distribution of the applied load, can be calculated from the recorded axial strain given the elastic modulus of the bar. For this study, 17 HPBs were utilised; one central bar and four arrays of four bars at 25 mm spacing, giving a 200 mm diameter instrumented area in the centre of the target plate.

## SOIL CONDITIONS

Eight tests were conducted in total; four with the explosive buried in saturated Leighton Buzzard (LB) sand, and four with the explosive buried in saturated Stanag soil. Leighton Buzzard is a relatively uniform, rounded to well-rounded quartz silica sand, named after the town in the UK where it is quarried. Stanag soil is a well-graded sandy gravel and is specified for use in buried charge tests in AEP-55 [10], and the UK testing annexe WP53308, based on STANAG 4569 [13] from where the soil gets its name.

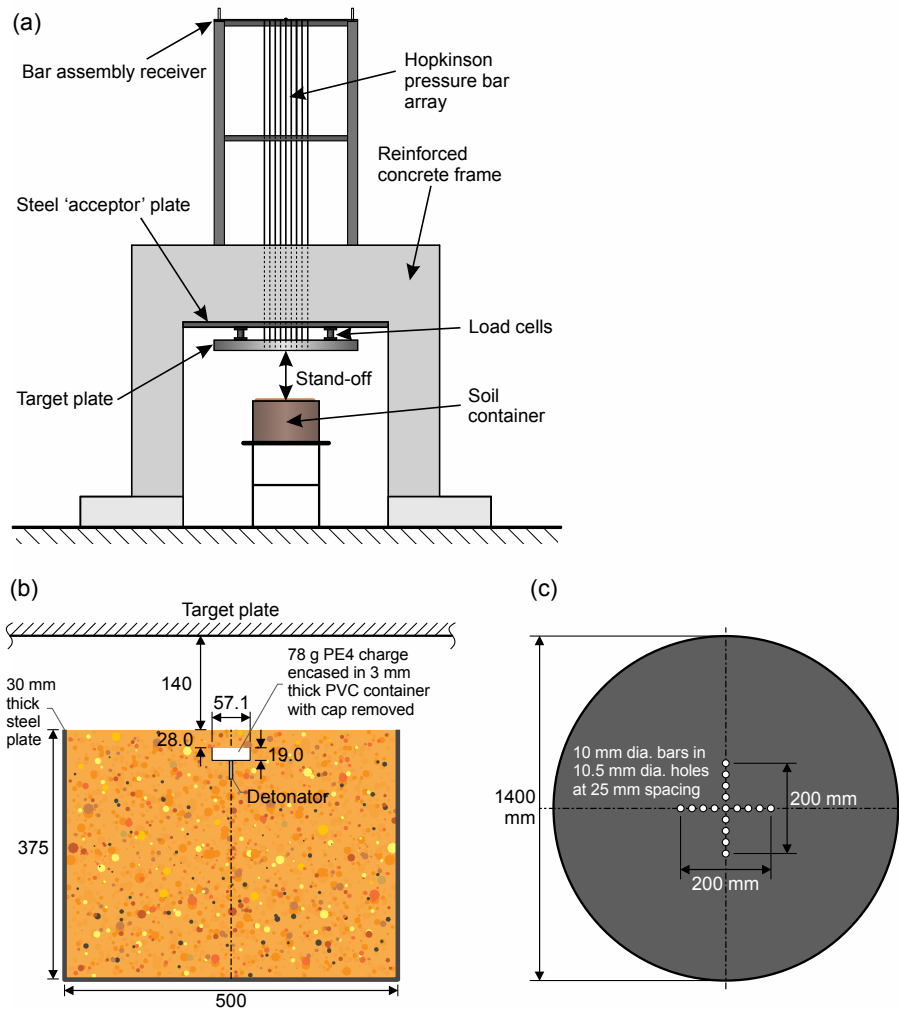


Figure 1: (a) Schematic of testing apparatus, (b) geometry of test arrangement, (c) Hopkinson pressure bar arrangement used in the test series [plan view]

Figure 2 shows the particle size distribution of the two soils. It can be seen that LB has a relatively tight banding, with particle sizes ranging between 0.6–1.18 mm. Conversely, the Stanag soil particle sizes range between <0.065–20 mm, with a small amount of fines (0.29% by mass) passing through the smallest (0.065 mm) sieve. In the current methodology, LB is compacted to give a bulk density of  $2.0 \text{ Mg/m}^3$  at full saturation, giving a dry density of  $1.60 \text{ Mg/m}^3$  and a therefore a saturated geotechnical moisture content of 25%, given as the mass of water divided by the dry mass of the soil. Because of the well-graded nature of Stanag soil, i.e. a greater proportional volume of fines, the soil has a lower natural porosity, and is compacted to give a bulk density of  $2.20 \text{ Mg/m}^3$  at full saturation, with a dry density of  $1.93 \text{ Mg/m}^3$  and a saturated geotechnical moisture content of 14%.

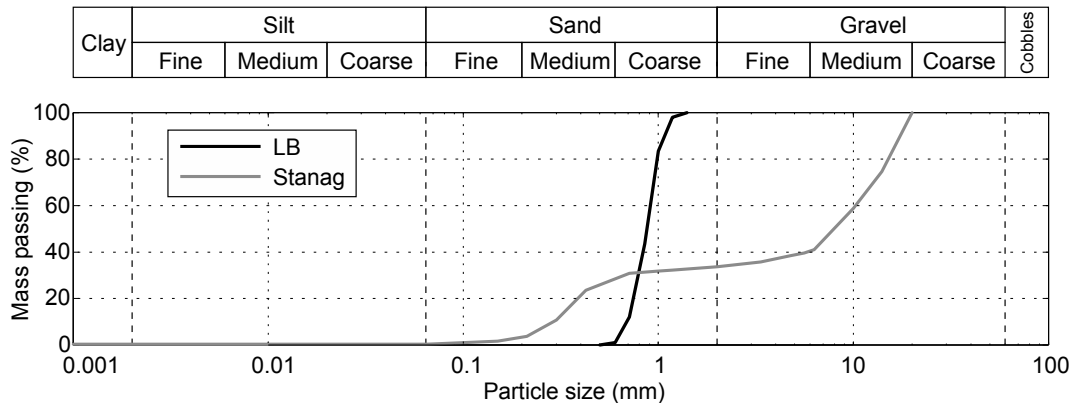


Figure 2: Particle size distributions for Leighton Buzzard (LB) and Stanag soil

### EXAMPLE RESULTS

For all tests presented in this paper, the data were recorded at 14-bit resolution with a sample rate of 1.56 MHz. The recording software was triggered via a voltage drop in a breakwire channel, with a new breakwire wrapped around the detonator for each test. The timebase of the pressure signals was shifted by  $50 \mu\text{s}$  to correct for the delay between the pressure acting on the face of the HPB and being recorded at the strain gauge location.

Figure 3 shows the pressure and specific impulse histories from a single test with the explosive buried to a depth of 28 mm in saturated LB, where the specific impulse was determined from cumulative numerical temporal integration of the recorded pressure histories. Each subplot shows signals from the bars located between 0 and 100 mm from the plate centre, in each of the  $-x$ ,  $+x$ ,  $-y$  and  $+y$  arrays respectively. The central 0 mm bar is common to all 4 arrays and hence is repeated in each subplot.

The peak pressure and peak specific impulse for the 50–100 mm bars *generally* appear to decay proportionally with distance from the plate centre (with a few exceptions here which are considered to be within acceptable experimental spread). The central bar and 25 mm bars appear similar in magnitude and form. As these five bars all lie within the projected area of the charge, it is likely that this is a feature of the charge geometry and that the central area of the target is loaded by a ‘flat-topped’ soil bubble. Future tests with buried spherical charges, although not corresponding to a threat level mandated in STANAG 4569, will confirm or deny this hypothesis.

The pressure history from saturated LB is indicative of the loading mechanism caused by the impact and lateral spreading of a highly pressurised fluid annulus, hypothesised by Grujicic [14] and recently confirmed in our experimental work [15]. As the expanding soil annulus propagates across the loaded face, the form of the imparted pressure becomes lower in magnitude and longer in duration, and at any instant in time there appears to only be a small area of the target being loaded, with the pressure traces returning to zero shortly after arrival, and passing, of the soil annulus. Qualitatively, there appears to be a good degree of bar-to-bar repeatability for both pressure and impulse.

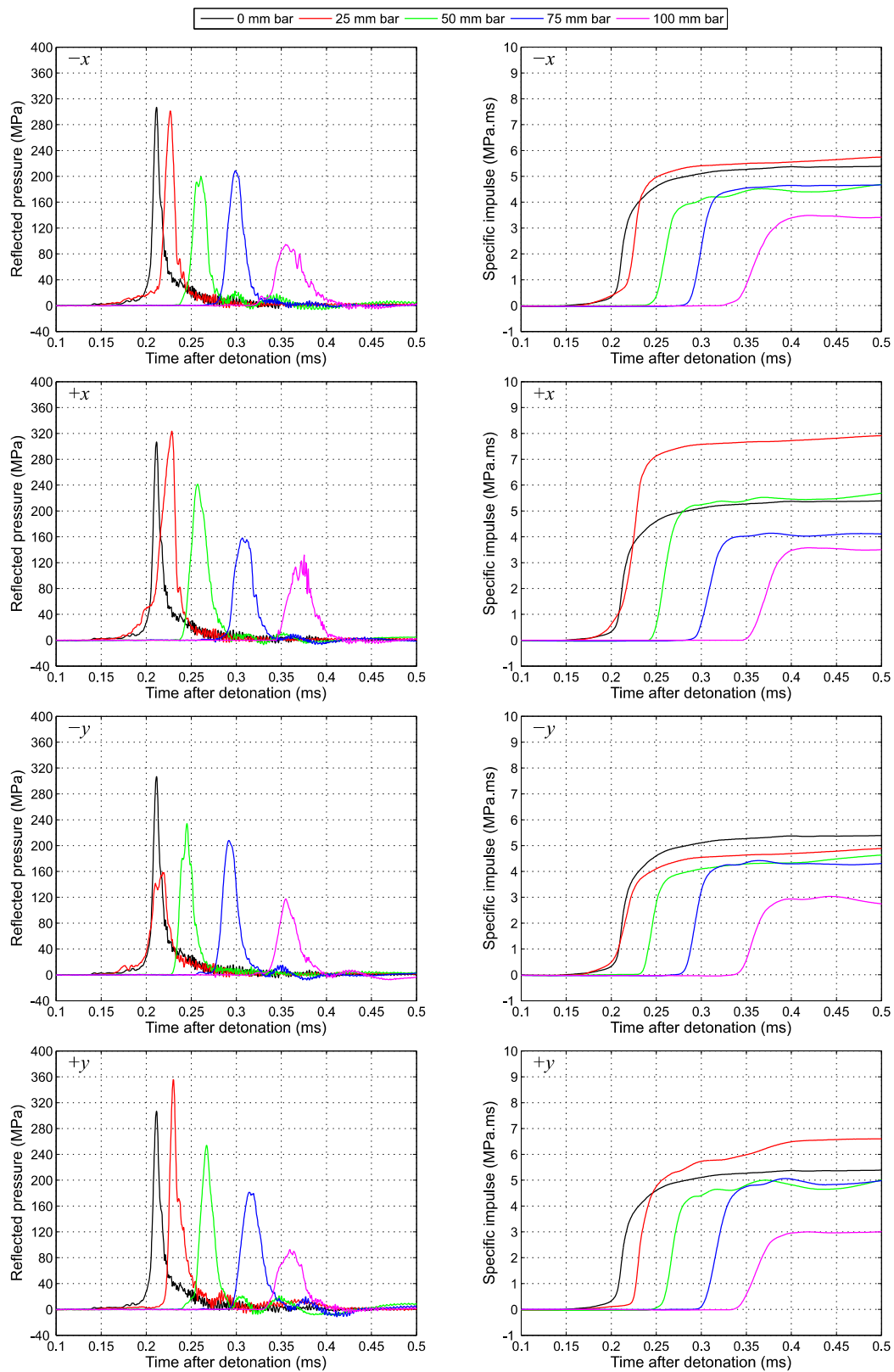


Figure 3: Example pressure-time and impulse-time histories for all 4 arrays, from a single test using saturated LB

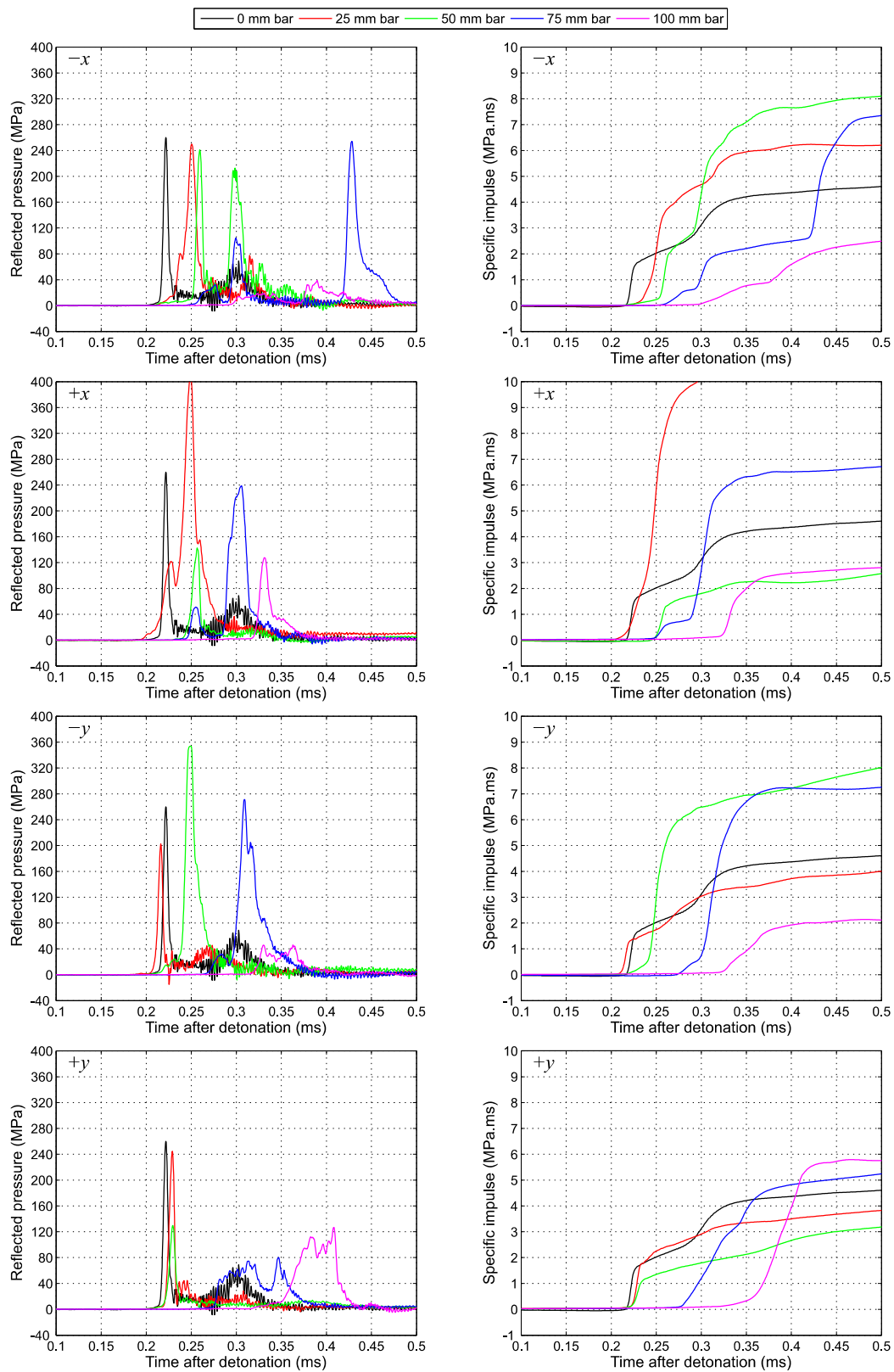


Figure 4: Example pressure-time and impulse-time histories for all 4 arrays, from a single test using saturated Stanag soil

Figure 4 shows the pressure and specific impulse histories from a single test with the explosive buried to a depth of 28 mm in saturated Stanag soil. It is immediately clear that the results are a) far more chaotic than the LB results, and b) the loading for any given bar appears more complex. Whilst the magnitudes are broadly similar in several cases, there are many instances of multiple loading. This can be seen as a ‘step-like’ impulse history, with the 75 mm bar in the  $-x$  array offering a clear example. Here, there is a small magnitude load acting between 0.25–0.3 ms, immediately followed by a secondary larger magnitude load, each imparting approximately 0.6 and 2.0 MPa.ms of specific impulse respectively. At around 0.42 ms after detonation there is a final phase of loading, equal in peak pressure magnitude and greater in specific impulse than the total loading on the central bar.

It is clear that the presence of a well-graded distribution of particle size within a soil causes a more complex and more stochastic loading mechanism to develop on the loaded face when compared to tests conducted with LB. Note that the largest particles in Stanag soil are twice the diameter of the recording HPBs rather than an order of magnitude smaller as with LB.

## COMPILED RESULTS

The peak reflected pressure, peak specific impulse and time to peak pressure were compiled for each test and are presented in Figure 5, separated into the two different soil types for clarity and ease of comparison. Here, the dashed line shows the mean value at each bar location across the entire test series. In previous work, time to peak pressure has been used as an analogue for arrival time as it offers a definitive data point that is less susceptible to sensor noise than, for example, estimating the time at which the pulse rises above zero [9]. It is clear that, because of the multiple loading feature present on several traces, the time to peak pressure for Stanag soil is no longer analogous to the arrival time. However, it is still a useful parameter for comparative purposes.

The mean peak pressure distribution is broadly similar for LB and Stanag soil, with the peak pressure varying from over 300 MPa in the area above the charge, to approximately 100 MPa at 100 mm from the plate centre. The peak specific impulse for LB is lower than the imparted impulse from the tests using Stanag soil, which is to be expected on account of the lower saturated bulk density of LB. It is also clear that for LB, the specific impulse imparted in the centre of the plate is substantially higher than the impulse imparted at the 100 mm bar location; the peak specific impulse decays by 50% from 6.8 MPa.ms at the centre to 3.4 MPa.ms at 100 mm. Conversely, the Stanag soil specific impulse distribution appears more uniformly distributed, with the specific impulse increasing from 7.5 MPa.ms at the central bar to 8.8 MPa.ms at the 75 mm bar, and subsequently decaying to 5.7 MPa.ms at the 100 mm bar location; a reduction of only 24% from the central bar value. The cause of the increase in mean specific impulse at 25 mm is presently unknown.

As with peak pressure, the mean time to peak pressure follows a similar trend for both soil types, with peak pressure for Stanag soil consistently arriving on average some 25  $\mu$ s later than the peak pressure for LB, at a given bar location. This can be explained by the larger bulk density and hence greater mass of soil being accelerated by the detonation products in the Stanag soil tests.

From examination of Figure 5, it is clear that the LB results occupy a narrow band on either side of the mean, whereas the Stanag soil results show a markedly increased variability. In order to quantify this, the relative standard deviation (RSD) was calculated for all data points measured at a given bar location for a given soil type. The RSD is expressed as a percentage of the mean, and

is plotted in Figure 6 for each soil for peak pressure and peak specific impulse at all bar locations. Here, while only four data points are used to calculate the central bar RSD, all subsequent RSDs at 25–100 mm are calculated from 16 data points, with four data points recorded in each of the four tests for that soil type.

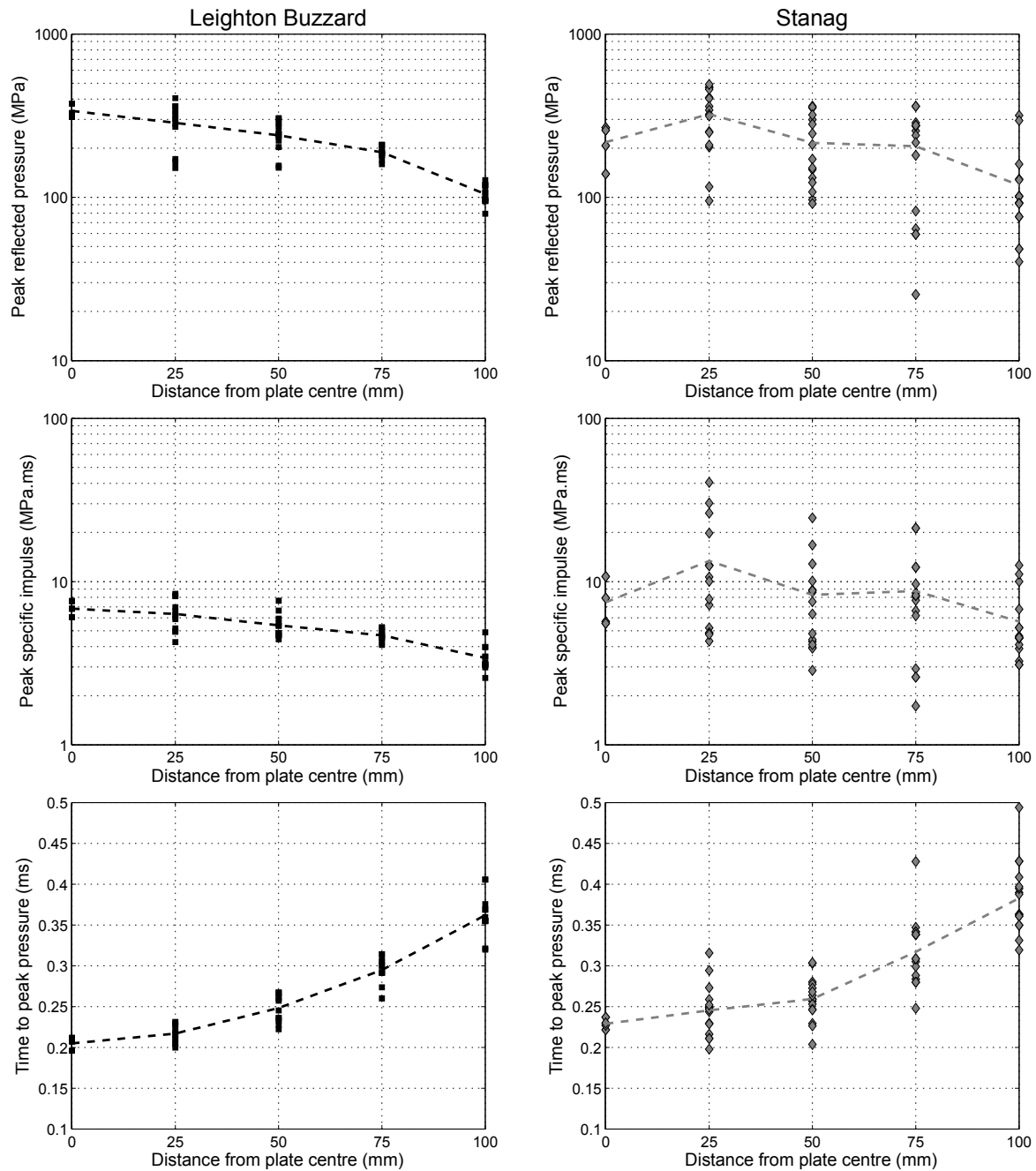


Figure 5: Compiled peak reflected pressure, peak specific impulse, and time to peak pressure for saturated LB and saturated Stanag soil

The maximum RSDs for Stanag soil are 67% for peak pressure and 79% for peak specific impulse. The localised variability for LB is considerably less, with peak values of 29% and 22% for peak pressure and peak specific impulse respectively; around a third of those for Stanag soil. Recent testing has confirmed that these variations are localised, and that global output remains relatively consistent [9].

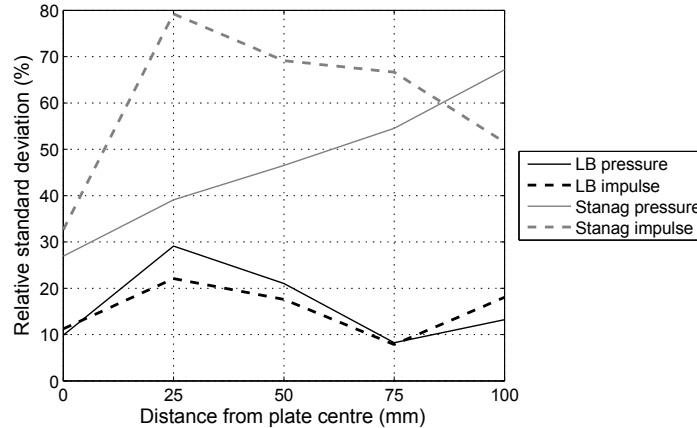


Figure 6: Relative standard deviation for peak reflected pressure and peak specific impulse for saturated LB and saturated Stanag soil

## DISCUSSION

It has been confirmed that the localised variations in loading from explosives buried in well-graded soils are substantially higher than those from explosives buried in uniform soils at this scale. Half-scale tests have shown that the total impulse imparted to a target is consistent, with a typical standard deviation of approximately 3% from the mean. [8]. This gives confidence that the variations of between 27% and 79% seen in the current testing are an intrinsic feature of the event itself, rather than being related to any experimental sources of error such as poor control of the geotechnical soil bed. Furthermore, these variations must be localised as they are not present in global impulse measurements and hence must even out over a sufficiently large loaded area.

As LB is a relatively uniform soil, the soil cap above the charge is given an effectively uniform velocity and expands as a regular, homogeneous soil bubble, impacting and spreading across the target in a repeatable manner and generally imparting a predictable loading distribution in both space and time. The soil bubble remains intact and retains the expanding detonation products, and hence the loading is predominantly in the form of a high velocity fluid (soil bubble) impact [15].

Conversely, Stanag soil has a large distribution of particle sizes and hence the momentum imparted to the soil cap is highly non-uniform. The loading appears to be a mixture of early-time fine particle impact, shock loading from the vented detonation products, and late-time impact of the larger particles in the soil cap. These larger particles impart a significant amount of impulse as they have been driven by the expanding detonation products for a longer duration and hence carry greater momentum than the early-time fine particles. The loading on any discrete HPB location is dictated by the size of particles directly beneath the bar, and hence is highly variable.

Despite this, the specific impulse decays more gradually with radial distance in the Stanag soil tests than in LB. This suggests that there is a greater level of total spatial uniformity arising from the global particle barrage associated with Stanag soil, ahead of the expanding soil annulus loading associated with the LB tests. This shows that whilst time-invariant measures of spatial distribution such as impulse plugs would show that Stanag soil produces more uniform loading conditions (i.e. the specific impulse distribution in Figure 5), it is only through measuring the spatial and temporal variation in loading that we can observe, and determine the physical cause for, localised spatial variations. The temporal distribution of loading is an important consideration for thin targets and/or targets with relatively short response duration, such as the undersides of armoured vehicles

This testing has highlighted clear difficulties in collecting reliable data from tests using Stanag soil when compared to more uniform soils such as LB.

## SUMMARY AND CONCLUSIONS

Eight tests have been conducted in total on explosives buried in saturated soils; four tests using uniform Leighton Buzzard sand and four tests using well-graded Stanag soil.

In each test, reflected pressure was measured at 17 locations within the central 200 mm diameter region of a rigid target plate using Hopkinson pressure bars, allowing the spatial and temporal distribution of loading to be recorded. The results clearly show that whilst LB produces repeatable data, tests using Stanag soil showed considerable spread in both the form and magnitude of the imparted pressure and specific impulse. This is as a direct result of the particle size distribution of the soil surrounding the charge.

It is hypothesized that uniform soils form a relatively uniform soil bubble that retain the detonation products and load the target in a typical fluid annulus manner. In non-uniform soils, the soil bubble ruptures early due to the differential momentum imparted to the fine and coarse particles situated in the soil cap. This gives rise to three distinct forms of loading; fine particle barrage, air shock from the vented detonation products, and coarse particle barrage. The latter imparts a substantially higher impulse due to the increased momentum imparted to the heavier particles which stay in contact with the un-vented detonation products for longer.

## ACKNOWLEDGEMENTS

This work forms part of the Dstl-funded *Characterisation of Blast Loading* project.

## REFERENCES

- [1] International Campaign to Ban Landmines – Cluster Munition Coalition. *Landmine Monitor*. 2015.
- [2] A. B. Wenzel and E. D. Esparza. *Measurement of pressures and impulses at close distance from explosive charges buried and in air*. Technical report, U.S. Army Mobility Equipment Research and Development Center, Fort Belvoir, Virginia, USA, 1972.
- [3] A. B. Wenzel and E. D. Esparza. *The response of armor plates to landmines using model experiments*. Technical report, U.S. Army Tank-Automotive Command (TACOM) Research and Development Center, Warren, Michigan, USA, 1974.

- [4] P. S. Westine, B. L. Morris, P. A. Cox, and E. Z. Polch. *Development of computer program for floor plate response from land mine explosions*. Technical Report 13045, U.S. Army Tank-Automotive Command (TACOM) Research and Development Center, Warren, Michigan, USA, 1985.
- [5] D. Bergeron, R. Walker, and C. Coffey. *Detonation of 100-gram anti-personnel mine surrogate charges in sand – a test case for computer code validation*. Technical Report 668, Defence Research Establishment Suffield, Ralston, Alberta, Canada, 1998.
- [6] L. C. Taylor, W. L. Fournery, and H. U. Leiste. Pressures on targets from buried explosions. *International Journal for Blasting & Fragmentation*, **4**(3):165–192, 2010.
- [7] S. D. Clarke, S. D. Fay, J. A. Warren, A. Tyas, S. E. Rigby, and I. Elgy. A large scale experimental approach to the measurement of spatially and temporally localised loading from the detonation of shallow-buried explosives. *Measurement Science and Technology*, **26**:015001, 2015.
- [8] S. D. Clarke, S. D. Fay, J. A. Warren, A. Tyas, S. E. Rigby, J. J. Reay, R. Livesey, and I. Elgy. Geotechnical causes for variations in output measured from shallow buried charges. *International Journal of Impact Engineering*, **86**:274–283, 2015.
- [9] S.E. Rigby, S.D. Fay, S.D. Clarke, A. Tyas, J.J. Reay, J.A. Warren, M. Gant, and I. Elgy. Measuring spatial pressure distribution from explosives buried in dry leighton buzzard sand. *International Journal of Impact Engineering*, **96**:89–104, 2016.
- [10] NATO. *Procedures for evaluating the protection level of logistic and light armoured vehicles. Allied engineering publication (AEP) 55, Vol. 2* (for Mine Threat), 2006.
- [11] A. Tyas, J. Warren, T. Bennett, and S. Fay. Prediction of clearing effects in far-field blast loading of finite targets. *Shock Waves*, **21**(2):111–119, 2011.
- [12] B Hopkinson. A method of measuring the pressure produced in the detonation of high explosives or by the impact of bullets. *Philosophical Transactions of the Royal Society of London. Series A, Containing Papers of a Mathematical or Physical Character*, **213**(1914):437–456, 1914.
- [13] NATO. Protection levels for occupants of logistic and light armoured vehicles. STANAG 4569, 24th May, 2004.
- [14] M. Grujicic and B. Pandurangan. A combined multi-material Euler/Lagrange computational analysis of blast loading resulting from detonation of buried landmines. *Multidiscipline Modeling in Materials and Structures*, **4**(2):105–124, 2008.
- [15] S. D. Clarke, S. E. Rigby, S. D. Fay, A. Tyas, J. J. Reay, J. A. Warren, M. Gant, R. Livesey, and I. Elgy. ‘bubble-type’ vs ‘shock-type’ loading from buried explosives. In: *Proceedings of the 16<sup>th</sup> International Symposium on Interaction of the Effects of Munitions with Structures (ISIEMS16)*, Florida, USA, 2015.